Hydrodynamic behavior in expanding thermal clouds of ^{87}Rb

I. Shvarchuck,[1] Ch. Buggle,[1] D. S. Petrov,[1,2] M. Kemmann,[1] W. von Klitzing,[1] G. V. Shlyapnikov,[1,2] and J. T. M. Walraven[1]
[1]*FOM Institute for Atomic and Molecular Physics, Kruislaan 407, 1098 SJ Amsterdam, The Netherlands*
[2]*Russian Research Center, Kurchatov Institute, Kurchatov Square, 123182 Moscow, Russia*
(Received 25 August 2003; published 4 December 2003)

We study hydrodynamic behavior in expanding thermal clouds of ^{87}Rb released from an elongated trap. At our highest densities the mean free path is smaller than the radial size of the cloud. After release the clouds expand anisotropically. The cloud temperature drops by as much as 30%. This is attributed to isentropic cooling during the early stages of the expansion. We present an analytical model to describe the expansion and to estimate the cooling. Important consequences for time-of-flight thermometry are discussed.

DOI: 10.1103/PhysRevA.68.063603 PACS number(s): 03.75.Hh, 03.75.Kk

I. INTRODUCTION

The anisotropic expansion of a condensate after release from a trap is one of the best known features of the Bose-Einstein condensed state [1,2]. The anisotropy arises because the condensate expands most rapidly in directions where it was originally most confined. The interest in this phenomenon is further growing, in particular since the observation of anisotropic expansions in noncondensed Bose gases [3,4] and in degenerate Fermi gases [5,6].

Anisotropic expansions are indicative for hydrodynamic behavior. It is well known that Thomas-Fermi condensates can be described by the classical Euler equation for potential flow of a nonviscous gas [7]. Therefore, they behave hydrodynamically even at very low densities. For classical clouds the situation is density dependent. At low densities, where the mean free path is large compared to the size of the cloud (collisionless regime), the expansion proceeds under free flow conditions (free expansion). The motion of the individual atoms is described by a single-particle Hamiltonian and the expansion is isotropic. Reducing the mean free path to a value smaller than the dimension of the cloud allows the introduction of a hydrodynamic field and leads to a crossover to hydrodynamic behavior (hydrodynamic expansion). Little difference is to be expected between the expansion of a condensate and that of a fully hydrodynamic thermal cloud [8]. Both the collisionless and the hydrodynamic regimes were studied theoretically (see Refs. [8–11], and references therein). Also the influence of mean-field effects [12] and the crossover between the two regimes were analyzed theoretically [13] and numerically [14].

It is important to understand the crossover to hydrodynamic behavior in thermal clouds. From the fundamental point of view it is important to quantify the hydrodynamic properties as these affect the coupling between condensates and thermal clouds. From the experimental point of view it is vital for the correct interpretation of time-of-flight absorption images of dense atomic clouds. Previously the crossover regime in thermal clouds was probed in experiments at MIT with a dense gas of ^{23}Na atoms [15] and at ENS using cold metastable triplet ^{4}He [16]. In Amsterdam the crossover regime was observed in experiments with ^{87}Rb [3]. Very pronounced hydrodynamic conditions were recently reached by exploiting a Feschbach resonance in fermionic gases [5,6,17–19]. Hydrodynamic behavior as observed in collective excitations is reviewed in Refs. [7,20].

In this paper we focus on hydrodynamic behavior as observed in the expansion of dense thermal clouds of ^{87}Rb, extending a brief analysis presented earlier in the context of the Bose-Einstein condensation formation experiments in Amsterdam [3]. The clouds are prepared in an elongated trap at a temperature T_0, just above the critical temperature for Bose-Einstein condensation. At the highest densities the mean free path is less than the radial size of the cloud. After release from the trap the clouds expand anisotropically and their temperature drops by as much as 30%. The behavior is intermediate between that expected for collisionless clouds, where cooling is absent, and pure hydrodynamic behavior, where the gas cools to vanishing temperatures.

We show that the expansion in axial direction is similar to that of a collisionless cloud at a temperature $T_z < T_0$. This "axial" temperature can be identified with the temperature T_* reached at the moment when the expansion ceases to be hydrodynamic and the cooling stops. Radially, the expansion proceeds faster than that expected for a collisionless cloud and can be characterized by a "radial" temperature $T_\rho > T_0$. For our conditions, the mean field of elastic interaction contributes $\sim 20\%$ to the total energy in the trap center. We show that this only has a minor effect (3%) on the expansion behavior. The consequences for time-of-flight thermometry are discussed.

II. EXPERIMENT

In our experiments we load a magneto-optical trap with approximately 10^{10} atoms from the source described in Ref. [21]. After optical pumping to the $|S_{1/2}, F=2, m_F=2\rangle$ state typically 4×10^9 atoms are captured in a Ioffe-Pritchard quadrupole magnetic trap. Then the gas is compressed and evaporatively cooled to a temperature just above T_C. The radio-frequency (rf) evaporation is forced at a final rate of $\dot{\nu}=-433$ kHz/s down to a value $\nu_1=740$ kHz, that is, 120 kHz above the trap minimum $B_0=88.6(1)$ μT as calibrated using atom laser output coupling [22]. As the final ramp down rate is $-\dot{\nu}/(\nu_1-\nu_0)\approx 4$ s^{-1}, i.e., slow compared to both axial and radial trap frequencies $\omega_z = 2\pi\times 20.8(1)$ s^{-1} and $\omega_\rho = 2\pi\times 477(2)$ s^{-1}, the evapora-

tion proceeds quasistatically and yields a sample characterized by a single uniform temperature and an equilibrium shape [23]. The preparation procedure is completed by 20 ms of plain evaporation at rf frequency ν_1. This procedure leaves us with $N=3.5(3)\times10^6$ atoms at density $n_0=3.6(6)\times10^{14}$ cm^{-3} in the trap center and temperature $T_0=1.17(5)$ μK.

A. Knudsen criterion

To establish the collisional regime we calculate the mean free path and the atomic collision rate. The mean free path in the trap center is given by the usual expression for a uniform gas [25] at density n_0,

$$\lambda_0=\frac{1}{\sqrt{2}n_0\sigma}\approx 3\ \mu\text{m}, \tag{1}$$

where $\sigma=8\pi a^2$ is the elastic-scattering cross section in the *s*-wave limit with $a=98.98(4)a_0$ the scattering length [26]. The atomic collision rate in the trap center is [25]

$$\tau_c^{-1}=\sqrt{2}n_0\bar{v}_{th}\sigma\approx 6000\ \text{s}^{-1}, \tag{2}$$

with $\bar{v}_{th}=(8k_BT_0/\pi m)^{1/2}$ as the thermal velocity.

The gas behaves as a hydrodynamic fluid if the mean free path is much smaller than the relevant sample size (Knudsen criterion). Defining the axial (l_z) and the radial (l_ρ) size parameters of the density profile in a harmonic trap, see Eq. (7), the Knudsen criterion can be expressed as

$$\frac{\lambda_0}{l_i}\simeq\omega_i\tau_c\ll 1, \tag{3}$$

with $i\in\{\rho,z\}$. For the axial direction the Knudsen criterion is very well satisfied, $\omega_z\tau_c\approx0.02$. For the radial direction we calculate $\omega_\rho\tau_c\approx0.5$. In this direction we operate in the middle of the crossover range between the collisionless and hydrodynamic regimes.

B. Time-of-flight analysis

In the crossover between hydrodynamic and collisionless conditions the time-of-flight analysis is nontrivial. Unlike in fully collisionless clouds, the velocity of the individual atoms is not conserved because the gas cools as it expands. Unlike in fully hydrodynamic clouds, cooling will only proceed during a finite period. Obviously, if the temperature drops during the expansion the question arises how to properly extract the temperature of the cloud from a time-of-flight absorption measurement.

In Fig. 1 we plot the measured axial and radial cloud sizes $l_z(t)$ and $l_\rho(t)$, as a function of expansion time *t*. All data were collected during a single run within 2.5 h, keeping track of some drift in the offset field [27]. Each data point corresponds to the average of about 20 measurements, with the error bars representing the standard deviation, typically 2% of the average value. The cloud sizes were determined with the usual procedure (see for instance Ref. [28]), i.e., the expression for the column density of an ideal Bose gas trapped in a harmonic potential

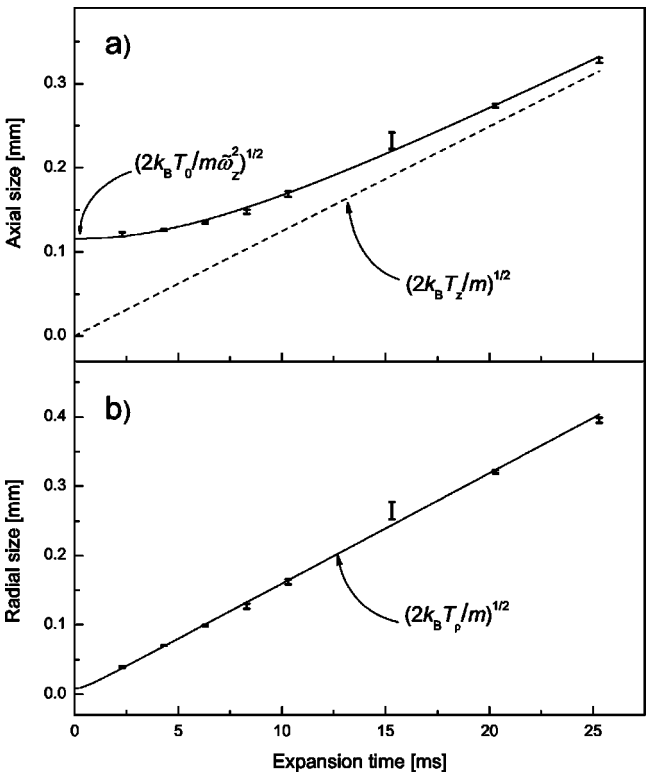

FIG. 1. Expansion measurements for (a) axial and (b) radial directions. The error bars represent two standard deviations. The solid lines represent Eqs. (9) and (10) with $l_z(t_*)=116$ μm, $T_z=0.83$ μK, and $T_\rho=1.35$ μK. Note the difference in vertical scale for the two panels. The dashed line represents the asymptotic expansion behavior in axial direction. As the initial radial size is very small the radial expansion is already asymptotic by the time the first data point is taken.

$$n_2(z,\rho)=n_{20}g_2[De^{-[z/l_z(t)]^2-[\rho/l_\rho(t)]^2}]/g_2[D] \tag{4}$$

is fitted, after transformation to optical density, to the images [29]. With this procedure we obtain values for the sizes $l_z(t)$ and $l_\rho(t)$, the degeneracy parameter (fugacity) *D*, and the peak column density n_{20} [30]. We use the notation $g_a[x]=\Sigma_{l=1}^{\infty}x^l/l^a$. The fugacity provides together with the initial sizes a self-calibrating method for the total atom number provided the average trap frequency $\bar{\omega}=(\omega_\rho^2\omega_z)^{1/3}$ is known,

$$N=g_3[D]\left(\frac{m\bar{\omega}}{2\hbar}\right)^3 l_z^2(0)l_\rho^4(0). \tag{5}$$

In practice only the axial size $l_z(0)$ is used because the aspect ratio is accurately known. The measured peak column density n_{20} is not used in our analysis [31].

Due to the presence of the elastic interactions between the atoms the density distribution will be slightly broadened and deformed [12,32]. Calculating the variance of the distribution $\langle z^2\rangle$ using the recursive expression for the density to first order in mean field $U_{\text{mf}}(\mathbf{r})=2gn(\mathbf{r})$ leads to

$$\tfrac{1}{2}m\omega_z^2 l_z^2(0) \simeq kT_0 + E_{\mathrm{mf}}, \tag{6}$$

where $E_{\mathrm{mf}} = g\int n^2(\mathbf{r})d\mathbf{r}/\int n(\mathbf{r})d\mathbf{r}$ is the trap averaged interaction energy with $g=(4\pi\hbar^2/m)a$ the interaction coupling constant [33]. The variance was related to the size parameter using $\langle z^2\rangle = \frac{1}{2}l_z^2(0)g_4[D]/g_3[D]$ [34]. Equivalently, treating the mean field as an effective potential we may write

$$\tfrac{1}{2}m\tilde{\omega}_z^2 l_z^2(0) = kT_0, \tag{7}$$

where $\tilde{\omega}_z$ represents a ''dressed'' trap frequency that reproduces, for an ideal gas at temperature T_0, the same cloud size,

$$\tilde{\omega}_i^2 = \omega_i^2(1-\xi), \tag{8}$$

where $\xi = E_{\mathrm{mf}}/(kT_0 + E_{\mathrm{mf}}) \approx 0.03$ [33].

To describe the expansion behavior analytically we introduce a schematic model in which the expansion is treated as purely hydrodynamic up to time $t=t_*$ and as purely collisionless beyond this point. At t_* the density has dropped to the level that no further collisions take place and the atomic velocities remain frozen. The axial expansion is represented by

$$l_z(t) \simeq [l_z^2(t_*) + (2k_B T_z/m)(t-t_*)^2]^{1/2}. \tag{9}$$

The presence of t_* slightly shifts the asymptote of the expansion curve. The radial expansion is asymptotic for all times relevant in the experiment,

$$l_\rho(t) \simeq [2k_B T_\rho/m]^{1/2} t. \tag{10}$$

In this case the shift of the asymptote is negligible. The parameters T_z and T_ρ represent apparent axial and radial temperatures corresponding to the asymptotic expansion velocities of the cloud in both directions,

$$s_i = \lim_{t\to\infty} \dot{l}_i(t) = (2k_B T_i/m)^{1/2}, \tag{11}$$

with $i \in \{\rho, z\}$. Note that Eqs. (9) and (10) reduce to the usual expressions for isotropic expansion of fully collisionless thermal clouds in the absence of a mean field when $t_* \to 0$ with $T_z = T_\rho = T_0$ (see, e.g., Ref. [28]).

III. RESULTS

Fitting Eq. (4) to our data, the degeneracy parameter was verified to be constant during the expansion to within experimental error $D=0.95(4)$. Once this was established we determined the cloud sizes by refitting all data with a fixed value $D=0.95$. The results are shown in Fig. 1 (solid bars). Fitting Eq. (9) to the results for the axial sizes we obtain the initial axial size $l_z(0) \simeq l_z(t_*) = 116(2)$ μm and the ''axial temperature'' $T_z = 0.83(4)$ μK. The fit is shown as the solid line in Fig. 1(a) and is insensitive to any reasonable choice of t_*. Fitting Eq. (10) to the radial data we obtain the solid line in Fig. 1(b), which corresponds to $T_\rho = 1.35(6)$ μK [35]. For all these results statistical errors are negligible. The quoted errors represent the uncertainty in the determination of the fugacity.

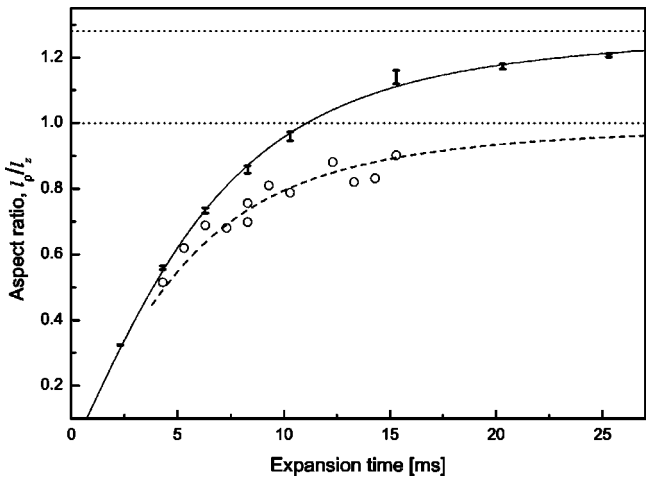

FIG. 2. Aspect ratio of a hydrodynamically expanding cloud as a function of expansion time. The error bars represent two standard deviations. The change from a cigarlike to a pancakelike shape is evident as the data points cross the value of $l_\rho/l_z = 1$. The open circles represent low-density clouds expanding isotropically. The solid and dashed lines represent fits of Eq. (35) to the data.

From the initial axial size we calculate with Eq. (7) $T_0 = 1.17(5)$ μK. Then, the central density $n_0 = 3.6(6) \times 10^{14}$ cm^{-3} follows with

$$n_0 = g_{3/2}[D]/\Lambda_0^3, \tag{12}$$

where $\Lambda_0 = [2\pi\hbar^2/mkT_0]^{1/2}$ is the thermal wavelength at temperature T_0. Using Eq. (8) to account for the mean-field broadening we calculate with Eq. (5) $N = 3.5(3)\times 10^6$ atoms. The error bar reflects the strict conditions on the atom number imposed by a known fugacity. We return to systematic errors in the section on thermometry.

The results presented here indicate a slightly decelerated expansion in axial direction, $T_z/T_0 = 0.71(2)$, and a slightly accelerated expansion in radial direction, $T_\rho/T_0 = 1.15(3)$. This corresponds to an ''inversion'' of the aspect ratio, which is demonstrated in Fig. 2 by plotting the aspect ratios for the same dataset as used in Fig. 1. At $t=12$ ms of expansion the cloud shape crosses over from a cigar shape to a pancake shape. The solid line represents a fit to the expansion model to be discussed below.

For collisionless samples the expansion is expected to be isotropic. This was verified by reducing the density by a factor of 30 (open circles in Fig. 2). In this case the expansion is indeed isotropic (dashed line), $s_z/s_\rho = 1.02(4)$.

IV. EXPANSION MODEL

To interpret our results for T_0, T_ρ and T_z we divide the expansion in two stages. During the first stage ($t<t_*$) the expansion is treated as purely hydrodynamic and is described by scaling theory [8,13]. All data are taken during the second stage ($t>t_*$) for which the expansion is treated as collisionless.

A. Hydrodynamic stage

During the hydrodynamic stage ($t<t_*$) we treat the expansion as isentropic, i.e., the gas cools while converting random motion into directed motion just as in the supersonic expansion of an atomic beam [36]. As for isentropic expansions the degeneracy parameter D is conserved [37] we find, using Eq. (12), that the temperature decreases according to

$$T(t)=T_0[n(t)/n_0]^{2/3}. \tag{13}$$

Turning to scaled size parameters, $b_i(t)\equiv l_i(t)/l_i(0)$ with $i\in\{\rho,z\}$, the density ratio is conveniently written as

$$\frac{n(t)}{n_0}=\frac{1}{b_\rho^2(t)b_z(t)}. \tag{14}$$

We note that for our elongated clouds ($\omega_z/\omega_\rho\ll 1$) the axial size remains practically unchanged during the early stages of the expansion. Therefore, setting $b_z=1$ in Eq. (14), the initial ($t\ll 1/\omega_z$) isentropic drop in temperature can be written as

$$T(t)/T_0=1/b_\rho^{4/3}(t). \tag{15}$$

Here $b_\rho(t)$ satisfies the scaling equations for expanding hydrodynamic thermal clouds [8] in the presence of a mean field [13]:

$$\ddot{b}_\rho=(1-\xi)\frac{\omega_\rho^2}{b_\rho^{7/3}b_z^{2/3}}+\xi\frac{\omega_\rho^2}{b_\rho^3 b_z}, \tag{16a}$$

$$\ddot{b}_z=(1-\xi)\frac{\omega_z^2}{b_z^{5/3}b_\rho^{4/3}}+\xi\frac{\omega_z^2}{b_\rho^2 b_z^2}. \tag{16b}$$

Equations (16a) and (16b) decouple for $t\ll 1/\omega_z$ since $b_z\simeq 1$. In this limit the radial scaling equation can be written as

$$\left(\frac{\dot{b}_\rho(t)}{\omega_\rho}\right)^2=\frac{3}{2}(1-\xi)[1-1/b_\rho^{4/3}(t)]+\xi[1-1/b_\rho^2(t)]. \tag{17}$$

We then substitute Eq. (17) into Eq. (15) and obtain to first order in $(\dot{b}_\rho/\omega_\rho)^2$ the temperature T_* reached at $t=t_*$:

$$\frac{T_*}{T_0}\simeq 1-\frac{2}{3}\left(\frac{\dot{b}_\rho}{\omega_\rho}\right)^2_{t=t_*}. \tag{18}$$

We point out that in the limit of very elongated clouds Eq. (17) also represents the correct description for a fully hydrodynamic expansion. Then, we may write for the asymptotic expansion velocity in radial direction

$$\lim_{t\to\infty}\frac{\dot{b}_\rho(t)}{\omega_\rho}=\frac{1}{\omega_\rho}\frac{s_\rho}{l_\rho(0)}=\sqrt{(1-\xi)\frac{T_\rho}{T_0}}. \tag{19}$$

Hence, comparing with the asymptotic value of Eq. (17) we conclude that the following inequality should hold:

$$1\leqslant T_\rho/T_0\leqslant 3/2+\xi. \tag{20}$$

Returning to our experimental conditions we emphasize that the duration of the hydrodynamic stage will be very brief because the instantaneous mean free path grows *quadratically* with b_ρ in these elongated clouds,

$$\lambda(t)/\lambda_0=b_\rho^2(t), \tag{21}$$

as follows with Eqs. (1) and (14) [38]. Roughly speaking t_* is reached when the mean free path equals the radial size of the cloud. Therefore, a rough estimate for t_* can be obtained by substituting $\lambda(t)=l_\rho(t)$ into Eq. (21) for $t=t_*$. With Eq. (3) this leads to

$$b_\rho(t_*)\simeq 1/\tilde{\omega}_\rho\tau_c. \tag{22}$$

As for $t\lesssim 1/\tilde{\omega}_\rho$ the radial size of a hydrodynamic cloud hardly differs from that of a collisionless cloud,

$$b_\rho(t)\simeq(1+\tilde{\omega}_\rho^2 t^2)^{1/2}, \tag{23}$$

we find with Eq. (22)

$$t_*\simeq(1/\tilde{\omega}_\rho)[(1/\tilde{\omega}_\rho\tau_c)^2-1]^{1/2}\approx 0.6\ \text{ms}. \tag{24}$$

A self-consistent estimate for our expansion model can be obtained by combining Eqs. (23) and (15) for $t=t_*$,

$$t_*\simeq(1/\tilde{\omega}_\rho)[(T_0/T_*)^{3/2}-1]^{1/2}. \tag{25}$$

However, for this estimate the ratio T_*/T_0 should first be established experimentally.

B. Collisionless stage

Once the expansion is ballistic ($t>t_*$) the variance of the axial ($i=z$) and radial ($i=\rho$) velocity components of the expanding gas can be written as

$$\langle v_i^2\rangle=\langle u_i^2\rangle+\langle w_i^2\rangle, \tag{26}$$

where u_i represents the thermal velocity components of the atoms and w_i the dynamic velocity components of the density distribution due to the expansion.

At the start of the ballistic stage ($t=t_*$) the thermal velocity components can be associated with T_*,

$$m\langle u_i^2\rangle=k_B T_*. \tag{27}$$

The dynamical velocities due to the overall expansion can be expressed as

$$m\langle w_i^2\rangle=m\langle\dot{r}_i^2\rangle=(\dot{b}_i/\tilde{\omega}_i)^2 k_B T_0=\tfrac{1}{2}m\dot{l}_i^2. \tag{28}$$

Here we used the scaling property $\dot{r}_i=(\dot{b}_i/b_i)r_i$, with the r_i representing the position coordinates in the expanding cloud. Since for collisionless clouds the $\langle v_i^2\rangle$ are conserved by the time the mean field has vanished, we may write

$$m\langle v_i^2\rangle=k_B T_i, \tag{29}$$

where the T_i are effective axial and radial temperatures that may be associated with the asymptotic axial and radial expansion velocities s_i defined in Eq. (11).

Substituting Eqs. (27) and (28) into Eq. (26) we obtain for $\xi \ll 1$

$$\frac{T_\rho}{T_0} = \frac{T_*}{T_0} + \left(\frac{\dot{b}_\rho}{\tilde{\omega}_\rho} \right)^2_{t=t_*} + \frac{\xi}{b_\rho^2(t_*)}, \tag{30}$$

where the second term on the right-hand side (rhs) represents both the hydrodynamic and mean field contributions to the dynamic motion at $t=t_* \ll 1/\omega_z$ and the third term the mean-field contribution to the dynamic motion for $t>t_*$ [39]. With Eq. (17) this results in the following relation between T_0, T_ρ, and T_* in expanding elongated thermal clouds:

$$\tfrac{3}{2} T_0 + \xi T_0 = \tfrac{1}{2} T_* + T_\rho . \tag{31}$$

This equation is valid for small mean fields provided $t_* \ll 1/\omega_z$ and expresses the energy conservation during the expansion. It implies

$$T_z = T_* . \tag{32}$$

This also follows directly by writing in analogy to Eq. (30)

$$\frac{T_z}{T_0} = \frac{T_*}{T_0} + \left(\frac{\dot{b}_z}{\tilde{\omega}_z} \right)^2_{t=t_*}, \tag{33}$$

taking into account that $(\dot{b}_z/\tilde{\omega}_z)^2$ is negligibly small [40].

V. THERMOMETRY

Result (32) shows that with our measurement of T_z we directly probe the temperature of elongated clouds at the end of the hydrodynamic stage. Knowledge of T_* allows us to obtain with Eq. (25) a self-consistent result for t_* within our expansion model. Using $T_*/T_0 = 0.71(2)$ we calculate $t_* = 0.28$ ms, somewhat smaller than the rough estimate (24).

Rewriting Eq. (31) we find an increase in the effective radial temperature:

$$\frac{T_\rho}{T_0} = \frac{3}{2}\left(1 - \frac{1}{3}\frac{T_*}{T_0} \right) + \xi = 1.18(2). \tag{34}$$

Hence 15% of the increase in T_ρ is due to the mean field. Note that Eq. (34) satisfies inequality (20). Notice further that the value $T_\rho = 1.37(6)$ μK obtained with Eq. (34) comes close to the value $T_\rho = 1.35(6)$ μK following directly from the radial expansion.

We found the fitting procedure for determining T_0, T_ρ, and T_* to be very sensitive for the detailed shape of the fit function. Choosing a simple Gaussian reduces the estimated values for these temperatures by as much as 25%. However, this enormous systematic error does not affect the corresponding aspect ratios by more than a few parts in a thousand. We found more indicators that the aspect ratios are more accurately determined than the absolute values. Interestingly, we find for the aspect ratios standard deviations of typically 1%, i.e., twice as small as for the absolute size [41]. This points to some form of error cancellation. Also the fit to the aspect ratio is somewhat better than those of the separate plots.

Let us now turn to the results for the aspect ratios as presented in Fig. 2. Using Eqs. (9), (10), and (31) the evolution of the aspect ratio can be expressed as

$$\frac{l_\rho(t)}{l_z(t)} \simeq \frac{[(\frac{3}{2}+\xi) - \frac{1}{2}(T_*/T_0)]^{1/2} \omega_z t}{[1 + \xi + (T_*/T_0)\omega_z^2 (t-t_*)^2]^{1/2}}, \tag{35}$$

where we presume $t \gg 1/\omega_\rho$ as in Eq. (10). By construction this form satisfies energy conservation. In this way our fitting function stays as close as possible to a fit to a solution of the scaling equations. Fitting Eq. (35) to the data using $\xi = 0.03$ and $t_* = 0.3$ ms we obtain $T_*/T_0 = 0.72(1)$. The fit is shown as the solid line in Fig. 2. The result agrees within experimental error with that obtained from the axial expansion data but the accuracy is slightly better. The method lacks the accuracy to extract ξ [42]. The dashed line in Fig. 2 corresponds to the collisionless limit of Eq. (35): $\xi = 0$, $t_* = 0$, and $T_* = T_0$.

Once Eq. (35) is accepted, time-of-flight information for a single expansion time suffices for thermometry. The procedure goes in two steps. First we set ξ and t_* equal to zero and use Eq. (35) to obtain a first estimate for T_*/T_0. With Eq. (34) T_ρ/T_0 follows. After T_ρ is determined from Eq. (10), we have an estimate for the absolute value T_0. Together with n_0, deduced from Eq. (12), this allows us to calculate ξ and t_*. Iterating the procedure once yields all values within the limits of accuracy of the analysis. Choosing the expansion time sufficiently long ($t \gg 1/\omega_z$) the results are very insensitive for the value of t_*.

Our estimates for the absolute values of T_0, T_ρ, and T_z are sensitive for the detailed shape of the clouds. Therefore, deviations from the Bose shape will result in systematic errors, in particular if the cloud shape changes during the expansion. Shape deviations can arise from the presence of the mean field. Also, inhomogeneous isentropic cooling as a result of the inhomogeneous density profile of our samples can give rise to deviations of the Bose shape. Further, it may be that our transformation from optical density to column density gives rise to slight distortions of the cloud shape as a result of optical pumping or saturation of the detection transition.

In our analysis we did not correct for deviations of the cloud shape from the Bose distribution. First of all because under our conditions the mean field is weak and our fits of Eq. (4) to the measured column densities look convincingly. Second, because shape deviations produce similar relative errors in all three temperatures. Therefore, they do not affect the conclusions and consistency of our analysis as long as the scaling approach remains valid.

VI. CONCLUSIONS

We studied the behavior of dense elongated clouds of ^{87}Rb in the crossover from the collisionless to the hydrodynamic regime. At our highest densities the mean free path is

slightly smaller than the radial size of the cloud and the expansion is anisotropic. The expansion can be described by a two-stage model in which the expansion is treated as purely hydrodynamic up to time $t=t_*$ and as purely collisionless beyond this point. We find that at the end of the hydrodynamic stage the temperature has dropped substantially due to isentropic cooling, $T_*/T_0=0.72(1)$. This reflects itself in an axial expansion that is substantially slower than expected for the collisionless case, $T_z=T_*$. In accordance with energy conservation the radial expansion is faster, $T_\rho>T_0$. The isentropic cooling is best determined from the aspect ratio. Although the mean field in the trap center is substantial, $U_{\mathrm{mf}}(0)/kT_0=0.23$, it hardly affects the expansion behavior. Including the mean field in the analysis only affects the value obtained for T_0, with T_z and T_ρ by definition being unaffected. In our case the mean-field corrections are too small to be extracted with a fitting procedure but can be calculated accurately. It leads to systematic errors in T_0 of order 3% if not included.

Presently it is possible to study the case of strong mean fields by tuning to a Feschbach resonance [5,6,17–19, 43,44]. It would be interesting to study the case where anisotropic expansions are to be expected, but the behavior of the system is dominated by the mean field rather than the collisional hydrodynamics.

ACKNOWLEDGMENTS

The authors wish to thank Paolo Pedri for stimulating discussions. This work was part of the research program on Cold Atoms of the Stichting voor Fundamenteel Onderzoek der Materie (FOM), which was financially supported by the Nederlandse Organisatie voor Wetenschappelijk Onderzoek (NWO). Further, the research received support from NWO under Project No. 047.009.010, from INTAS under Project No. 2001.2344, and from the Russian Foundation for Basic Research (RFBR).

[1] M.H. Anderson, J.R. Ensher, M.R. Matthews, C.E. Wieman, and E.A. Cornell, Science **269**, 198 (1995).
[2] K.B. Davis, M.-O. Mewes, M.R. Andrews, N.J. van Druten, D.S. Durfee, D.M. Kurn, and W. Ketterle, Phys. Rev. Lett. **75**, 3969 (1995).
[3] I. Shvarchuck, Ch. Buggle, D.S. Petrov, K. Dieckmann, M. Zielonkowski, M. Kemmann, T. Tiecke, W. von Klitzing, G.V. Shlyapnikov, and J.T.M. Walraven, Phys. Rev. Lett. **89**, 270404 (2002).
[4] F. Gerbier, J.H. Thywissen, S. Richard, M. Hugbart, P. Bouyer, and A. Aspect, e-print cond-mat/0307188.
[5] K.M. O'Hara, S.L. Hemmer, M.E. Gehm, S.R. Granade, and J.E. Thomas, Science **298**, 2179 (2002).
[6] T. Bourdel, J. Cubizolles, L. Khaykovich, K.M.F. Magalhães, S.J.J.M.F. Kokkelmans, G.V. Shlyapnikov, and C. Salomon, Phys. Rev. Lett. **91**, 020402 (2003).
[7] L. Pitaevskii and S. Stringari, *Bose-Einstein Condensation* (Clarendon Press, Oxford, 2003).
[8] Yu. Kagan, E.L. Surkov, and G.V. Shlyapnikov, Phys. Rev. A **55**, R18 (1997).
[9] A. Griffin, W.C. Wu, and S. Stringari, Phys. Rev. Lett. **78**, 1838 (1997).
[10] D. Guéry-Odelin, F. Zambelli, J. Dalibard, and S. Stringari, Phys. Rev. A **60**, 4851 (1999).
[11] U. Al Khawaja, C.J. Pethick, and H. Smith, J. Low Temp. Phys. **118**, 127 (2000).
[12] D. Guéry-Odelin, Phys. Rev. A **66**, 033613 (2002).
[13] P. Pedri, D. Guéry-Odelin, and S. Stringari, Phys. Rev. A **68**, 043608 (2003).
[14] H. Wu and E. Arimondo, Europhys. Lett. **43**, 141 (1998).
[15] D.M. Stamper-Kurn, H.J. Miesner, S. Inouye, M.R. Andrews, and W. Ketterle, Phys. Rev. Lett. **81**, 500 (1998).
[16] M. Leduc, J. Leonard, F.P. Dos Santos, E. Jahier, S. Schwartz, and C. Cohen-Tannoudji, Acta Phys. Pol. B **33**, 2213 (2002).
[17] S. Jochim, M. Bartenstein, G. Hendl, J.H. Denschlag, R. Grimm, A. Mosk, and M. Weidemüller, Phys. Rev. Lett. **89**, 273202 (2003).
[18] S. Gupta, Z. Hadzibabic, M.W. Zwierlein, C.A. Stan, K. Dieckmann, C.H. Schunck, E.G.M. van Kempen, B.J. Verhaar, and W. Ketterle, Science **300**, 1723 (2003).
[19] C.A. Regal and D.S. Jin, Phys. Rev. Lett. **90**, 230404 (2003).
[20] F. Dalfovo, S. Giorgini, L.P. Pitaevskii, and S. Stringari, Rev. Mod. Phys. **71**, 463 (1999).
[21] K. Dieckmann, R.J.C. Spreeuw, M. Weidemüller, and J.T.M. Walraven, Phys. Rev. A **58**, 3891 (1998).
[22] I. Bloch, T.W. Hänsch, and T. Esslinger, Phys. Rev. Lett. **82**, 3008 (1999).
[23] The excitation of a quadrupole oscillation by the procedure of forced evaporation [3,24] can give rise to spurious anisotropies in the expansion and should be avoided. We verified this point explicitly: the aspect ratio, measured after 8 ms of expansion, was found to be constant to within experimental error (1%) as a function of plain evaporation time.
[24] I. Shvarchuck, Ph.D. thesis, University of Amsterdam, 2003 (unpublished).
[25] S. Chapman and T.G. Cowling, *The Mathematical Theory of Non-Uniform Gases* (Cambridge University Press, Cambridge, 1970).
[26] E.G.M. van Kempen, S.J.J.M.F. Kokkelmans, D.J. Heinzen, and B.J. Verhaar, Phys. Rev. Lett. **88**, 093201 (2002).
[27] A positive deviation in T_0, due to drift in the offset field B_0, translates itself directly into positive deviations of both l_z and l_ρ. We measured a positive B_0 drift of 0.6 μT/h (4 kHz/h). As the final frequency of rf evaporation, ν_1, is kept constant, this corresponds to a -3.3%/h drift in the well depth and a comparable negative drift of T_0. To minimize errors of this type B_0 was reset half way the measurements by a -0.7 μT offset field adjustment. This increases l_z and l_ρ by about 2%, i.e., still within one standard deviation, as was confirmed by measuring l_z and l_ρ before and after the B_0 correction. In plotting the aspect ratio errors of this type—at least partially—cancel.
[28] W. Ketterle, D.S. Durfee and D.M. Stamper-Kurn, in *Making, Probing and Understanding Bose-Einstein Condensates*, Pro-

ceedings of the International School of Physics ''Enrico Fermi,'' Course CXL, edited by M. Inguscio, S. Stringari, and C. Wieman (IOS Press, Amsterdam, 1999).

[29] Detection is done on the $|S_{1/2},F=2\rangle \rightarrow |S_{3/2},F=3\rangle$ transition at various detunings, depending on the density. The light intensity is 2 mW/cm^2. The laser polarization is linear. The effects of saturation and optical pumping arise only at small detunings and are corrected for to first order where necessary.

[30] We observe our samples under an angle of 73° with respect to symmetry axis of our trap. This can be accounted for by a straightforward correction that depends on the aspect ratio. The correction is 4.5% for our largest aspect ratios and accurate to within 10%. This means that it introduces only a small ($<1\%$) systematic error in the determination of T_0.

[31] The peak density determination based on the optical cross section agrees within a factor of 2 with the value based on the fugacity.

[32] V.V. Goldman, I.F. Silvera, and A.J. Leggett, Phys. Rev. B **24**, 2870 (1981)

[33] For a Gaussian cloud at temperature T_0 the trap-averaged interaction energy is given by $E_{\rm mf}=gn_0(2\sqrt{2})^{-1}$. For a Bose gas at $D=0.95$ the interaction energy is $\sim 25\%$ smaller. Substituting the numerical values obtained for n_0 and T_0 we calculate $\xi \simeq E_{\rm mf}/kT_0 \approx 0.03$. This result has an accuracy of the order of the expansion parameter $(2gn_0/kT_0)\approx 0.22$.

[34] In using this relation only the broadening of the Bose distribution is taken into account and not its deformation.

[35] Our optical resolution is 3.3 μm (1/e half-width) as measured with a positive 1951 USAF resolution target on the 6.9-μm periodic stripe pattern. This is much smaller than the radial size at 2.3 ms of expansion. We also verified that ''lensing'' is negligible: for the detuning and the densities present at 2.3 ms of expansion we can approximate our sample by a thin cylindrical lens with a focal length of 10^4 times its radial size.

[36] *Atomic and Molecular Beam Methods*, edited by G. Scoles (Oxford University Press, New York, 1992).

[37] For a harmonic trap the entropy is given by the expression $S=Nk_B(4g_4[D]/g_3[D]-\ln D)$.

[38] This is the case for constant cross section. Note that near a scattering resonance the unitarity limit may be reached, where $\sigma=8\pi/k^2$ with k the relative momentum between the colliding atoms. Then we have $\lambda(t)/\lambda_0=b_\rho^{2/3}(t)$ and the gas becomes *more hydrodynamic* during the expansion until ultimately the unitarity condition $ka\gg 1$ breaks down due to cooling of the gas cloud.

[39] Here we presume elongated clouds, so that the mean field can be transferred to the dynamic motion on a time scale short in comparison to the axial frequency, $t\ll 1/\omega_z$.

[40] Solving the scaling equations (16a) and (16b) for the axial expansion with $b_z=1$ for $t\lesssim 1/\omega_\rho$ yields the following approximate result: $\dot{b}_z/\omega_z \simeq \sqrt{2}(\omega_z/\omega_\rho)[b_\rho-1]^{1/2}$. For $t=t_*$ we calculate $(\dot{b}_z/\tilde{\omega}_z)^2=2(1-\xi)(\omega_z/\omega_\rho)^2[(T_0/T_*)^{3/4}-1] \approx 2\times 10^{-3}$.

[41] Here the low-density data represented by the open circles in Fig. 2 are left outside consideration.

[42] Fixing only the freezing time $t_*=0.3$ ms the fitting procedure yields $\xi=0.0(1)$ and $T_*/T_0=0.71(4)$.

[43] S. Inouye, M.R. Andrews, J. Stenger, H.-J. Miesner, D.M. Stamper-Kurn, and W. Ketterle, Nature (London) **392**, 151 (1998).

[44] S.L. Cornish, N.R. Claussen, J.L. Roberts, E.A. Cornell, and C.E. Wieman, Phys. Rev. Lett. **85**, 1795 (1998).